




# Strain-sensitivity conductive MWCNTs composite hydrogel for wearable device and near-infrared photosensor

Ran An<sup>1</sup>, Baoming Zhang<sup>1</sup>, Linglin Han<sup>1</sup>, Xiangdong Wang<sup>1</sup>, Yulin Zhang<sup>1</sup>, Lingying Shi<sup>1</sup>, and Rong Ran<sup>1,\*</sup> 

<sup>1</sup> College of Polymer Science and Engineering, Sichuan University, Chengdu 610065, China

**Received:** 13 November 2018

**Accepted:** 11 February 2019

**Published online:**

25 February 2019

© Springer Science+Business Media, LLC, part of Springer Nature 2019

## ABSTRACT

Healable, flexible, near infrared sensitive and strain-sensitive for wearable device and healthcare monitoring are successfully formed from sensitive, conductive and biocompatible hydrogels. In this work, a sensitive, mechanically self-healing hydrogel was fabricated via the incorporation of multiwalled carbon nanotubes (MWCNTs) into the hydrophobically associated polyacrylamide hydrogels. As a result, the optimal tensile strength (0.91 MPa) and electrical conductivity ( $0.5 \text{ S m}^{-1}$ ) were achieved for the PAM/MWCNTs composite hydrogels. Due to its various functions, the cross-linking hydrogel could be made as a strain sensor. The strain sensor achieved a gauge factor of 5.6, and its response time was 0.3 s. It could be stretched at least for 200 cycles, which was further applied to monitor human movement, including movement of the hands, elbow and even swallowing. With excellent mechanical properties, tensile sensitivity and biocompatibility, the prepared hydrogels could be used as a perfect material for electronic skin. At the same time, flexible and healable PAM/MWCNTs hydrogel had a sensitive near-infrared light response, and we create a new flexible and healable near-infrared light-sensitive photosensor because of the incorporation of MWCNTs, which is different from the traditional NIR photosensor. It could be used in NIR detector, medical instrument and health equipment.

## Introduction

The development of flexible electronic devices is in urgent need of soft conductors with multiple functions simultaneously, such as mechanical properties

(stretchability, toughness, flexibility and self-healing properties) and conductivity [1–5]. Particularly, a stretchable sensor is needed to maintain stable electrical conductivity while stretching for large deformations to produce next generation of portable wearable electronics, such as stretchable

Address correspondence to E-mail: ranrong@scu.edu.cn

sensor or energy storage devices [6–8]. Unfortunately, the materials which are used currently as conductors (such as metals, nanofibers, carbon-based materials and conductive polymers) are hard or finite stretch, and especially, the electrical properties would deteriorate rapidly under deformation [9, 10]. As a semi-solid ionic conductor, hydrogel has attracted extensive interest in the field of flexible electronics due to its advantages of viscoelasticity, adjustable property and good biocompatibility [3, 4, 11–13]. Furthermore, the conductivity of hydrogels-based ionic conductors can be maintained under stretching conditions, which is different from the hard and non-retractable electronic conductors [3, 4].

In addition, multiwalled carbon nanotubes (MWCNT) composite hydrogels have great potential in biomedical engineering [5], due to their excellent electrical conductivity and remarkable mechanical properties. Despite the MWCNT composite hydrogels have made some achievement, there are still challenges to be faced. The poor dispersion of MWCNTs in water has always been a significant problem in the preparation of composite hydrogels. Due to the effect of van der Waals gravity between individual pipes, the dispersity of MWCNTs in hydrogels is weakened, leading to the reduction in conductivity and mechanical properties [6]. In addition, the weak interfacial interaction between MWCNTs and organic polymer matrix limits the payload transfer to polymer, thus limiting the enhancement of MWCNTs in nanocomposites. Modifying carbon nanotubes with functional groups is an effective way to improve the dispersion of MWCNTs and strengthen the interaction with polymer network interface, so as to enhance the physical properties of composite hydrogel [7]. However, how to effectively graft oxygen-containing groups onto the surface of MWCNTs without damaging the structure is still an urgent problem to be solved.

Near-infrared photodetection is valuable for numerous scientific, industrial and recreational applications. And enhanced detectivities, improved flexibility and lower manufacturing costs are targeted towards scientific, industrial and communal applications [8]. More specifically, the detection of wavelengths in the near-infrared (NIR) region (800–3000 nm) [11] is appealing for applications ranging from industrial inspection and sorting, to safety, security and life sciences [12–14]. MWCNTs have excellent conductive, thermal sensitivity and

NIR sensitivity. In past research, MWCNTs conductive hydrogel has not been used in NIR detector. Due to its remarkable flexibility and self-healing ability, PAM/MWCNTs composite hydrogel could be constructed as a simple NIR photosensor to detect near-infrared light sources rapidly.

Considering, electrically conductive hydrogels with excellent self-healing abilities show a good application prospect in strain sensors [15–18], drug delivery vehicle [19] and electronic skin [20–26]. In this work, the multifunctional conductive HA hydrogels with desirable mechanical property and self-healing ability were fabricated by the incorporation of MWCNTs into the hydrophobically associated (HA) polyacrylamide hydrogel. We used modified Hummers' method to modified MWCNTs, which had better hydrophilic ability compared to other MWCNTs used in composite hydrogels. It could be placed stably for at least 6 months without precipitation and dissolved in some common solvent, which expanded the range of application of our modified MWCNTs. The cross-link network of the hydrogel obtained in this work is hydrophobic association, which can largely improve the self-healing ability of hydrogel. In our work, we improve the self-healing ability and mechanical properties at the same time through adding modified MWCNTs in HA hydrogels, which are difficult to achieve simultaneously in other gel-based biosensors. And we further developed their potential applications in strain sensors, human movement sensor and near-infrared photosensor which are not discussed in previous MWCNTs composite hydrogels. We used HCT<sub>x</sub> hydrogel to represent the prepared PAM/MWCNTs hydrogel, where *x* represented the ratio of the mass of MWCNTs to the volume of the AM (w/v%). The chemical structure, morphology, electrical conductivity, photothermal behaviour, mechanical properties and self-healing abilities of the hydrogels were systematically evaluated. The dispersion of MWCNTs modified by Hummers' method was more uniform than unmodified MWCNTs (b-MWCNTs). The HCT hydrogels displayed a high conductivity of 0.5 S m<sup>-1</sup>. In addition, we designed a simple and wearable device to detect the movements of human fingers to demonstrate their excellent sensitivity, conductivity and flexibility. Due to the stretching super-sensitivity of the HCT hydrogels, the device could detect very small movements. Also, the HCT hydrogels were very sensitive to near-infrared (NIR)

light, and the temperature would increase rapidly in just a few seconds. Furthermore, we creatively designed a simple NIR photosensor which is flexible and healable. And it can be used in medical device to detect the NIR source around human body and process locally heated treatment. Cytotoxicity tests showed that they were not toxic to cardiomyocytes. All of these results indicated that these self-healing and multifunctional hydrogels exhibited great potential for application in intelligent sensors and wearable electronic devices.

## Experimental section

### Materials

Multiwalled carbon nanotubes (MWCNTs) was provided by Chengdu Organic Chemicals Co. Ltd. Acrylamide (AM) (degree of alcoholysis = 98–99% mol/mol), sodium dodecyl benzene sulfonate (SDBS) and stearyl methacrylate (SMA) were purchased from Aladdin Industrial Corporation. Potassium persulfate (KPS) was purchased from Kelong Chemical Reagent Factory (Chengdu, China). Deionized water was provided by Chengdu Changzheng Chemical Reagent Co., Ltd. All of these above-mentioned reagents were used as received.

### Synthesis of modified MWCNTs

Modified MWCNTs were obtained from exfoliation of high purity MWCNTs in acidic medium by a modified Hummers' method. Briefly, a mixture of 6 g of MWCNTs, 3 g of  $\text{NaNO}_3$  and 140 mL of  $\text{H}_2\text{SO}_4$  was placed in a flask cooled in an ice bath, and the mixture was kept stirring until total homogenization. After that, 18 g of  $\text{KMnO}_4$  was gradually added to the solution while stirring. Next, the solution was removed from the ice bath to 35 °C. After that, the solution was added 280 mL deionized water and heat up to 95 °C for 0.5 h. The mixture was washed with an aqueous solution (500 mL) of 3 wt%  $\text{H}_2\text{SO}_4$  and 0.5 wt%  $\text{H}_2\text{O}_2$  for three times. The solid product obtained after the rigorous cleaning process was rinsed using copious amounts of distilled water. Finally, the resulting modified MWCNTs were dried by lyophilization in order to obtain a non-agglomerated dried powder.

### Hydrogel preparation

In this work, polyacrylamide (PAM)/MWCNTs hydrophobically associated hydrogels were fabricated through a simple and effective in situ polymerization. Exactly, the surfactant SDBS (5 wt% to the total weight), a certain mass of MWCNT and 20 ml deionized water were continuously magnetically stirred for 1 h first and then sonicated for 1 h. Next, hydrophilic monomer AM (20 wt% to the total weight) was incorporated into the stirring MWCNT dispersion, and then, the hydrophobic monomer SMA (2 wt% to the total weight) was added into the system. Also, the initiator KPS solution (0.5 wt% relative to the total mass of SMA and AM) was added into the mixture. Then, the mixture was added to a mould and placed at 50 °C for 4 h. Finally, HCT hydrogels samples were obtained. Moreover, the pure HA hydrogel was fabricated through the same preparation process for comparison.

## Results and discussion

### Dispersion of MWCNTs

The dispersion of MWCNTs and unmodified MWCNTs in different solvents is shown in Fig. 1. Briefly, 10 mg of unmodified MWCNTs (b-MWCNT) and MWCNTs are dispersed in 10 ml of deionized water, acetone and ethanol, respectively. After 1-h ultrasonic processing, these solutions are placed for 5 min, 1 h and 5 h. Obviously, MWCNTs show excellent dispersion in all of the three solvents even for 5 h when the b-MWCNTs precipitate in these solvents (Fig. 1a–c). The reason is that the carboxyl groups grafted on the surface of MWCNTs strengthen the electrostatic repulsion between MWCNTs and combine it with water. The homogeneously dispersed MWCNTs solution is favourable for the preparation of homogeneous HCT hydrogels.

To prove that the hydrophilic groups are surely connected to MWCNTs, the chemical structure of the b-MWCNTs (unmodified MWCNTs) and MWCNTs is characterized by FT-IR spectra (Fig. 2a). From the curve of MWCNTs, typical peaks at  $3438\text{ cm}^{-1}$  are assigned to O–H stretching vibration and  $1637\text{ cm}^{-1}$  correspond to C=O stretching vibration. And the peak at  $1060\text{ cm}^{-1}$  corresponds to the C–O–C stretching vibration. These groups prove that there

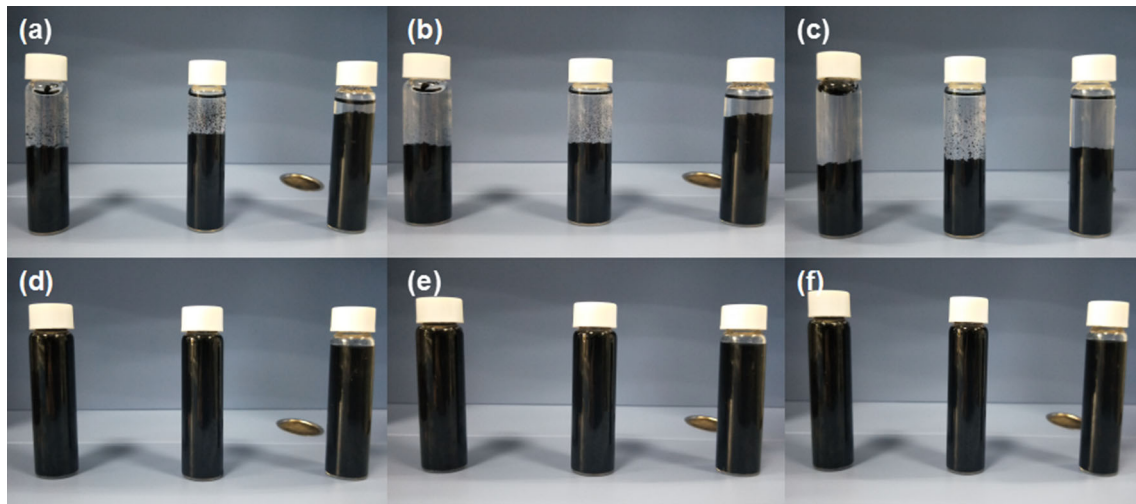
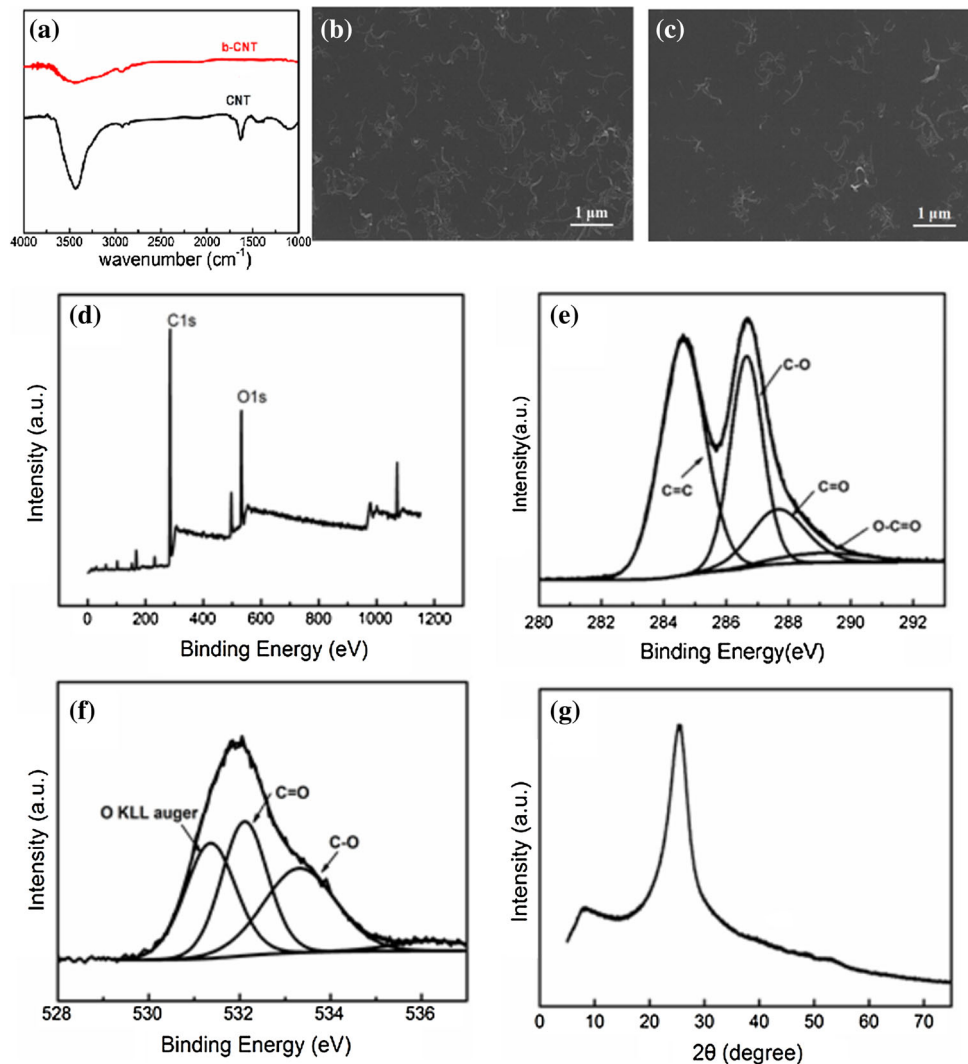


**Figure 1** Photographs of b-MWCNTs placed for 5 min (a), 1 h (b) and 5 h (c) in water, ethanol and acetone after ultrasound for 1 h; photographs of MWCNTs placed for 5 min (d), 1 h (e) and 5 h (f) in water, ethanol and acetone after ultrasound for 1 h.

**Figure 2** a Carbon nanotubes before and after the hydrophilic modification. SEM photographs of b-CNT (b) and MWCNTs (c) dispersed in water; d the survey XPS data of CNT; e the corresponding high-resolution spectrum of C 1s; f the corresponding high-resolution spectrum of O 1s; g the XRD spectrum of the modified carbon nanotubes.



are a large number of hydroxyl and carboxyl groups on the surface of MWCNTs. And b-MWCNTs do not have these hydrophilic groups. The dispersion of b-CNT and modified MWCNTs is directly characterized by SEM. As shown in Fig. 2b–c, it is obvious that modified MWCNTs could disperse uniformly in the water, indicating that oxygen groups successfully grafted on the surface of MWCNTs and the hydrophilic modification by modified Hummers' method could efficiently promote the uniformity of MWCNTs. As shown in Fig. 2d, XPS is applied to investigate the internal structure of MWCNTs, where the O 1s peak intensity has significantly increased for modified MWCNT. The C 1s spectra and O 1s spectra are presented in Fig. 2e–f, and the peak intensities associated with oxygen-containing components of modified MWCNTs are obvious. It was determined that oxygen-containing groups were grafted onto MWCNTs.

It can be seen that there is a sharp diffraction peak when  $2\theta = 26^\circ$ . The layer spacing is calculated as 0.34 nm according to the Bragg equation, which shows that the central structure of MWCNTs layer has not been changed and the hydrophilic groups are only grafted on the surface of MWCNTs.

### Morphology and structure

SEM micrographs showed that all of the obtained hydrogels represent porous structure, which allows large deformation of hydrogels (Fig. 3). As for HA hydrogel, its large and uneven pore size manifests a loose structure (Fig. 3a) and the diameters of pores are about 85  $\mu\text{m}$ . In contrast, when MWCNTs were incorporated into the HA hydrogel matrix, the pore size become small and uniform, which not only makes the structure much denser but also establishes the conductive pathway. It is worth noting that the pore sizes decrease first and then increase with incremental contents of MWCNTs (Fig. 3b–f), and the minimum diameter is 45  $\mu\text{m}$  when the content of MWCNTs is 2 wt%. The reason is that the low concentration of MWCNTs acts as physical cross-linking points, leading to the smaller and more uniform pore size. But when the MWCNTs are added too much, they will reunion and damage the structure of the HA hydrogel. Therefore, adding appropriate content of MWCNTs could obtain uniform and dense porous structure and further improve the performance of these composite hydrogels.

### Mechanical property

Due to the homogeneous MWCNTs dispersion, the obtained HCT hydrogels with different MWCNTs contents are fabricated through one-pot polymerization (Fig. 4b) and the schematic diagram is shown in Fig. 4a. It is worth noting that it was difficult to incorporate the AM and SMA into the MWCNT dispersion and fabricate composite hydrogels successfully when the MWCNTs loading was higher than 5 wt%. The reason was that the high total mass of MWCNT would result in high viscosity dispersion after ultrasonic treatment. The HCT hydrogels have great resistance to large deformation such as knotting (Fig. 4c), knotted stretching (Fig. 4d) and convolving (Fig. 4e), indicating that the HCT hydrogels have excellent flexibility. As shown in Fig. 4f, the HCT hydrogel could be stretched to 960% of its original length. The results indicate that the HCT hydrogel has excellent flexibility and mechanical properties compared to HA hydrogel. From what has been discussed above, the prominent stretchability, excellent flexibility and remarkable restorability would helpfully broaden the scope of application of HCT hydrogels.

The tensile mechanical property of the HCT hydrogels plays a significant role in their practical applications. Normally, the fracture energy and the tensile stress of HA hydrogel are not more than 0.777 MJ/m<sup>3</sup> and 0.064 MPa, respectively. As shown in Fig. 5a–b, after the incorporation of MWCNTs, the strength and toughness of HCT hydrogel are greatly improved. The HCT<sub>2</sub> hydrogel exhibits the highest mechanical properties with fracture energy of 7.635 MJ/m<sup>3</sup> and tensile strength of 0.908 MPa. The reason is that the hydrophilic group on the MWCNTs not only connects with water but forms the hydrogen bond with AM, which can construct a compact network and support more strength. But adding redundant content of hydrophilic MWCNTs will destroy the hydrophobic association interaction and the internal structure of network, leading to the weakness of the mechanical properties. But on the whole, adding MWCNTs can enhance both tensile strength and toughness compared to HA hydrogels due to the excellent mechanical properties of MWCNTs.

Figure 5c–d illustrates the compressive test of the HCT hydrogels with varied contents of MWCNTs. Similar to the tensile strength tests described above,

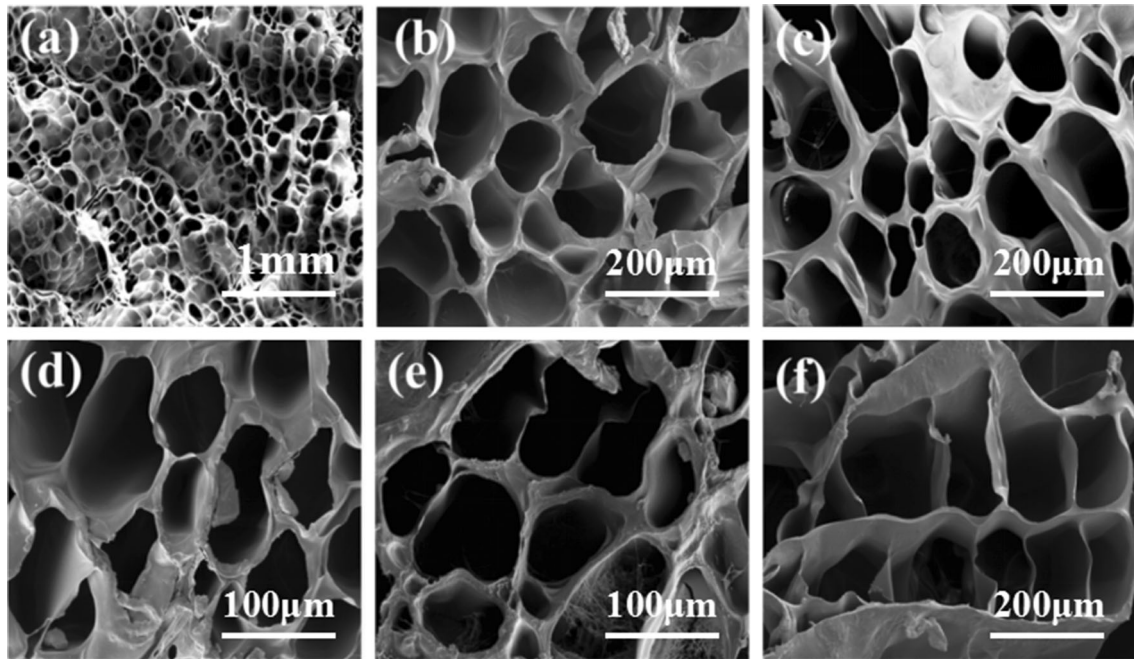


**Figure 3** a SEM overall images of HA gel, b–f SEM images of HA, HCT<sub>1</sub>, HCT<sub>2</sub>, HCT<sub>4</sub>, HCT<sub>5</sub> hydrogels in high magnification, respectively.

the compressive strength vs contents of MWCNTs curve has a peak as well, due to the reunion of MWCNTs at the high contents. The HCT<sub>2</sub> hydrogel achieves the maximum compressive strength of 1.466 MPa, which is almost four times higher than HA hydrogel of 0.4 MPa.

The tensile loading–unloading curves to explore the recovery properties of the HCT hydrogels at room temperature are tested. As shown in Figure S1(a–b), loading–unloading stress–strain curves are repeated with different contents of MWCNTs at the fixed strain of 300%. All gel samples have an obvious hysteresis loops, but hysteresis loops of HCT hydrogels are larger than HA hydrogel. Significantly, the hysteresis loops have a largest value when the content of MWCNTs is 2 wt%. The main reason is that the MWCNTs with larger content dissipated most of the energy when the hydrogels received external force. The tensile loading–unloading test indicated that the HCT hydrogels exhibited better mechanical properties than HA hydrogel.

To further research the fatigue resistance of HCT hydrogels, continuous cyclic loading–unloading curves at the fixed strain of 300% for the 2 wt% HCT gel (Figure S1-c) were tested. We calculated dissipated energies through the hysteresis loops shown in Figure S1-d. It was observed that the first cycle

showed the largest hysteresis loop, confirming a high ability to dissipate energy. It is evident that the hysteresis loop becomes much smaller in the following successive four loading–unloading cycles. The reason is the hydrogen bond is destroyed by the action of the applied load. All of the results indicate rapid recovery and fatigue resistance property of the HCT hydrogels.

Also, the intermittent cyclic tensile test of HCT<sub>2</sub> hydrogel is shown in Figure S1-e. The HCT<sub>2</sub> hydrogel was strained after waiting for 0 min, 5 min, 10 min, 30 min and 60 min, respectively. In particular, the tensile stress of HCT<sub>2</sub> hydrogel increased significantly with incremental waiting time. The reason may be that the stretching process of MWCNTs would make them orientate along the drawing direction after a certain time and then, it could carry more external force [27]. Since the disorientation is a process of entropy increase, the oriented polymer will return to its original shape without external tensile stress. Because hydrogel contains a large amount of water, there will be water loss after long-term placement, which will affect its recovery. However, when the waiting time is too long, HCT hydrogels could not restore to original deformation. The results of the intermittent cyclic tensile tests

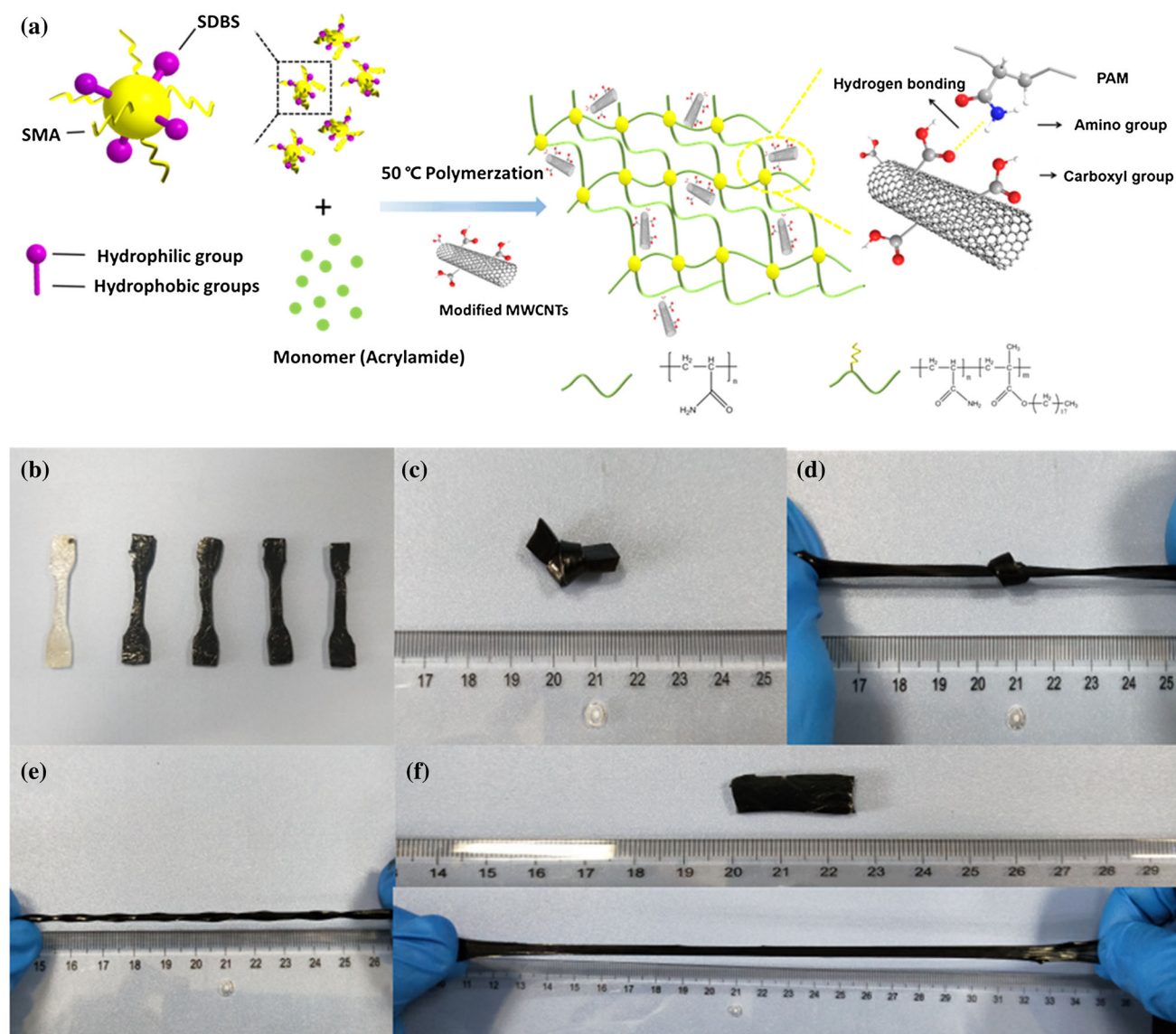


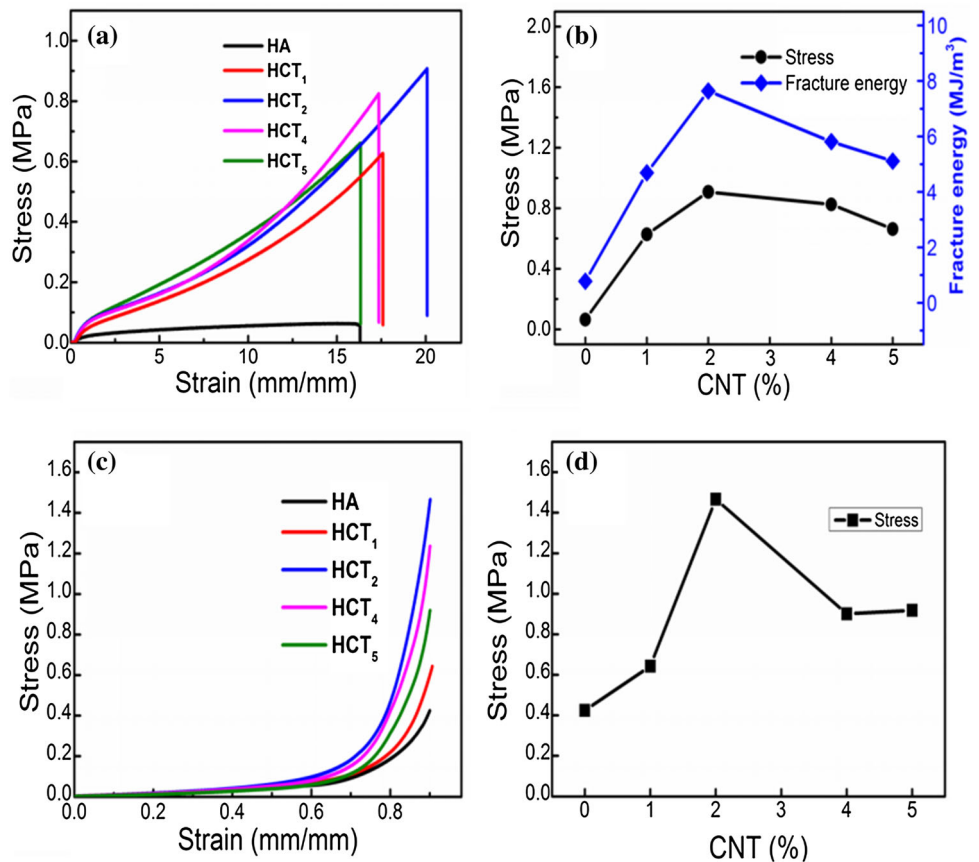
**Figure 4** a Schematic diagram of HCT hydrogel; b photograph of the HCT hydrogels; the deformation of knotting (c), knotted stretching (d), twisted (e) and stretching for 840% (f).

showed that the HCT hydrogels could enhance its mechanical properties effectively after a certain time.

HA gel is a single physical cross-linking network, and its swelling stability is poor (Figure S5a). After swelling in deionized water for 3 days, it breaks down and its structure disintegrates, failing to maintain its gel shape. But after adding the modified MWCNTs, the HCT hydrogels show good stability of swelling, which could reach the swelling equilibrium about 5 days and remain stable in 2 weeks or so in deionized water. As shown in Figure S5b, HA gels' swelling ratio is 98, while HCT1, HCT2, HCT4 and HCT5 hydrogels' swelling ratio is 31, 15, 20 and 24,

respectively. Compared with pure HA gel, the density of HCT hydrogel network increased, so the swelling ratio decreased. However, the overall environment became more hydrophilic after the overdose of modified MWCNTs, which destroyed the cross-linking point of hydrophobic association. The swelling property of hydrogels is an important property in the application of hydrogels. HCT hydrogels can maintain a stable shape in the underwater environment for a long time, which is conducive to the operation of sensors underwater.

**Figure 5** **a** Tensile stress–strain curves with different contents of MWCNTs and **b** tensile stresses and fractured energy curves versus MWCNTs contents; **c** compressive stress–strain curves with different contents of MWCNTs and **d** compressive stresses versus MWCNTs contents.



## Electrical conductivity

The variations of the conductivities of HCT hydrogels with different MWCNTs are shown in Figure S2. Similar to other composite hydrogels containing MWCNTs, the incremental MWCNT contents will gradually improve the conductivity of these hydrogels. As shown in Figure S2, the conductivity value is quite low ( $0.1 \text{ S m}^{-1}$ ) for HA hydrogel while the HCT<sub>5</sub> hydrogel has the highest value of  $0.5 \text{ S m}^{-1}$ , which indicated that the incorporation of MWCNTs could significantly improve the conductivity of HCT hydrogel. The reason is that incremental MWCNTs contents would produce more contact between MWCNTs, subsequently increase the content of conductive pathways and further improve the conductivity of HCT hydrogels. In the following tests, HCT<sub>5</sub> hydrogel is used to conduct a series of electrical tests to get the most efficient results.

To prove that the HCT hydrogels have high strain sensitivity, ultrafast response and excellent electrical stability to construct strain sensor, a tensile loading–unloading test is used in the electric circuit. As shown

in Figure S3, the brightness of the LED bulb reduced gradually when the strain deformation of HCT hydrogel increases from 0 to 200%, indicating that the conductivity of hydrogels is highly sensitive to stretching. Figure 6a displays the curves of the relative resistance for the hydrogels with clear step-like trend during a step-by-step loading–unloading cycle. Moreover, when the hydrogel is loaded and unloaded to certain strain deformation, the relative resistance rose and fell without lag, which verified the ultrafast response ability. Furthermore, the relative resistance of the hydrogels remains at a constant value during the load-holding or unload-holding process, indicating excellent electrical stability. To construct the wearable device, the sensitivity of the hydrogel was tested, which is defined as gauge factor ( $GF = (\Delta R/R_0)/\varepsilon$ , where  $\varepsilon$  is the tensile strain), varying from  $4.02 \pm 0.124$  to  $5.67 \pm 0.142$  as the strain changes from 50 to 200% (Fig. 6b), indicating that the strain sensor has a relatively high sensitivity. Table S1 illustrates the strain sensing performance of some conductive composites reported previously. According to Table S1, the gauge factor value of our



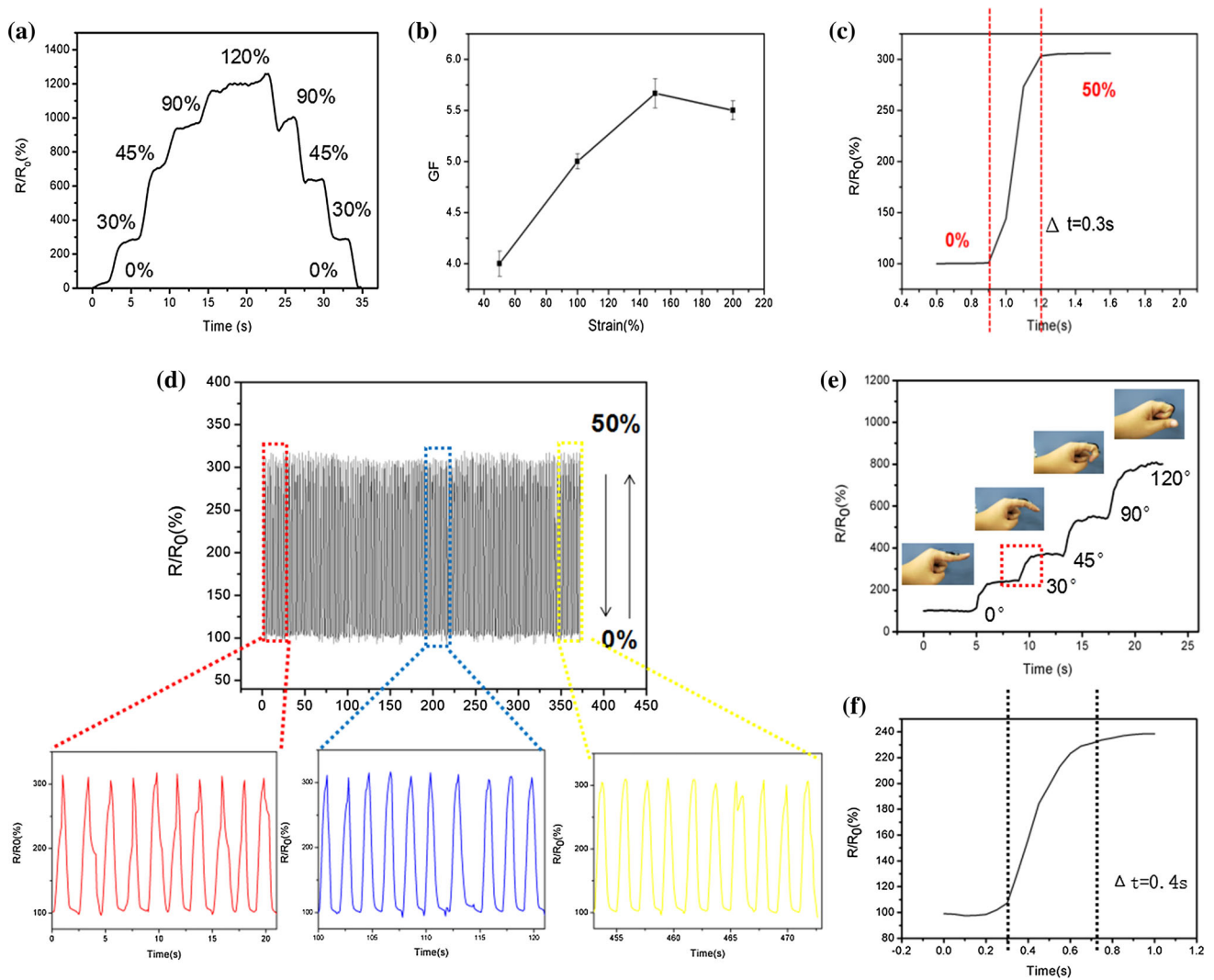


**Figure 6** **a** The resistance changes ( $R/R_0$ ) versus time under different tensile strains; **b** the gauge factor changes under different tensile strains; **c** the response time ( $\Delta t$ ) of strain sensor under 50% tensile strains; **d** relative resistance variation of the HCT hydrogel under continuous stretch and release from 0 to 50% strains for 370 s ( $\sim 200$  cycles); **e** the recorded resistance variations of the

HCT hydrogel strain sensors adhered onto the finger bending with different angles. The insets show the photographs of HCT hydrogel strain sensors adhered onto the finger bending at different angles; **f** the response time ( $\Delta t$ ) of strain sensor bending at  $30^\circ$ .

work is higher than that reported for other conductive nanocomposite systems. To further prove the reliability of the hydrogels, 200 tensile cycles under 50% strain are applied. As shown in Fig. 6d, after 200 cycles, the relative resistance of the hydrogel without deformation is still the same as the initial state, which indicates that HCT hydrogels have excellent durability and circularity. In the process of repeated stretching, a peak is chosen randomly to calculate the response time (Fig. 6c). The valley is denoted as the initial test time  $t_0$ , and the peak is denoted as the end time  $t_1$ . Therefore, the response time  $\Delta t$  of HCT

hydrogels for the tensile deformation is defined as  $\Delta t = t_1 - t_0$ . The response time measured during repeated stretching is 0.3 s, indicating that the HCT hydrogels have high sensitivity and fast responsibility. Then, the strain sensor is attached to person's finger, and a step-like trend can be observed with different bend angles. The fingers' bending behaviour at different angles can be accurately reflected by monitoring resistance changes (Fig. 6e). As shown in Fig. 6f, the response time ( $\Delta t = 0.4$  s) of finger indicates the fast rapid response of HCT hydrogels for wearable devices and electronic skin.

The flexibility, as a soft thermal response material in practical application in wearable devices, has been further examined. The HCT hydrogel can be bent into a crimp deformation by using small external stress, and it is used as an electrical conductor to light a LED bulb. Even if the device has a large torsion angle of  $360^\circ$ , the light of LED bulb is almost unchanged, revealing the insensitivity of HCT hydrogel to torsion. As shown in Figure S4, the relative resistance of HCT hydrogel basically is maintained at a certain level, but only it shows a small variation of 2.9% when the twist angle increased from  $0^\circ$  to  $720^\circ$ , demonstrating excellent flexibility, high mechanical adaptability and remarkable electrical stability.

The conductive HCT hydrogel can be constructed as a wearable device for detecting human motion. Figure 7 demonstrates that the wearable strain sensor is constructed by connecting the HCT hydrogel to electrical wire and the corresponding signals are recorded with an analyzer. They are adhered to the fingers, throat, opisthenar and elbow joint through adhesive tape. Due to the sensitivity to small vibration, the HCT hydrogels can also check the health of person's throat by attaching to it (Fig. 7a). Figure 7b–d shows the change in relative resistance of strain sensors when opisthenar and elbow joints bend with different directions, proving the sensing reliability of strain sensors. As shown in Fig. 7c, the HCT hydrogel-based wearable sensor is attached to the finger through adhesive tape. When the finger bent at different time intervals like 5 s, 2 s and 1 s, the strain sensor was replied rapidly. Furthermore, the sensor could monitor and quantify the real-time strain change. At the same time, no obvious allergic reactions, redness or skin injuries are observed during monitoring, indicating the outstanding biocompatibility of the HCT hydrogels-based strain sensor. Therefore, the HCT hydrogel-based strain sensor could be well performed when adhered to the body, which is advantageous for real-time monitoring of personal healthcare.

### Photothermal properties of hydrogels triggered by near-infrared (NIR) light

It is reported that conductive nanomaterials or polymers such as MWCNTs have the ability to absorb near-infrared light and convert it into heat effectively. Hence, it is viable that hydrogels with these nanomaterials of polymers can show photothermal

properties when these conductive components are incorporated into hydrogels. As shown in Fig. 8a, the photothermal behaviour of hydrogels with different MWCNTs contents is tested. The temperature change is not obvious when the laser irradiates HA hydrogel. But all HCT hydrogels exhibit rapid and notable temperature variations when the laser intensity is only  $0.8 \text{ W/cm}^2$ . This result shows that the hydrogels have excellent near-infrared sensitivity and can be used as sensor materials. The temperature changes were  $0^\circ\text{C}$ ,  $85^\circ\text{C}$ ,  $110^\circ\text{C}$ ,  $122^\circ\text{C}$  and  $140^\circ\text{C}$  for HA, HCT<sub>1</sub>, HCT<sub>2</sub>, HCT<sub>4</sub> and HCT<sub>5</sub> hydrogels in 42 s, respectively. All the temperature changes of HCT hydrogels are divided into two stages. In the process of 0–35 s, the temperature rises very rapidly. The curve become gently in the process of 35–42 s. With the increase in MWCNTs content, the temperature change is faster and the final temperature increases (Fig. 8b). As shown in Fig. 8c, we also used the infrared imager to detect the temperature rise of HCT hydrogels. Obviously, with incremental MWCNTs contents, the heating rate of the HCT hydrogels become higher and the response rate become faster when the HCT hydrogels are exposed to laser light at the same time.

Conductive HCT hydrogel has excellent near-infrared light response, and its resistance changes after exposing to infrared light. A near-infrared light-sensitive photosensor could be constructed by HCT hydrogels. As shown in Fig. 8c, when the HCT hydrogel is irradiated by near-infrared light, the resistance of HCT light-sensitive sensor decreases. After removing the near-infrared light source, the resistance gradually increases and can be restored to its original level. Furthermore, the enhanced ion dissociation at elevated temperature also leads to the increased concentration of charge carriers [28]. The resistance of the HCT light-sensitive sensor decreases monotonically with incremental irradiated time under all strains. The variations of resistances of stretchable HCT light-sensitive sensors is different in relaxed (0% strain) and stretched (100%, 200% strain) state. As shown in Fig. 8d, the photothermal sensitivity of HCT hydrogels increases with incremental strain deformation. The reason may be that the surface area of HCT hydrogel-based light-sensitive sensors exposed to heat increases under stretching, which enables more efficient heat adsorption and increases the response. Furthermore, the alignments of both polymer chains and ionic conduction

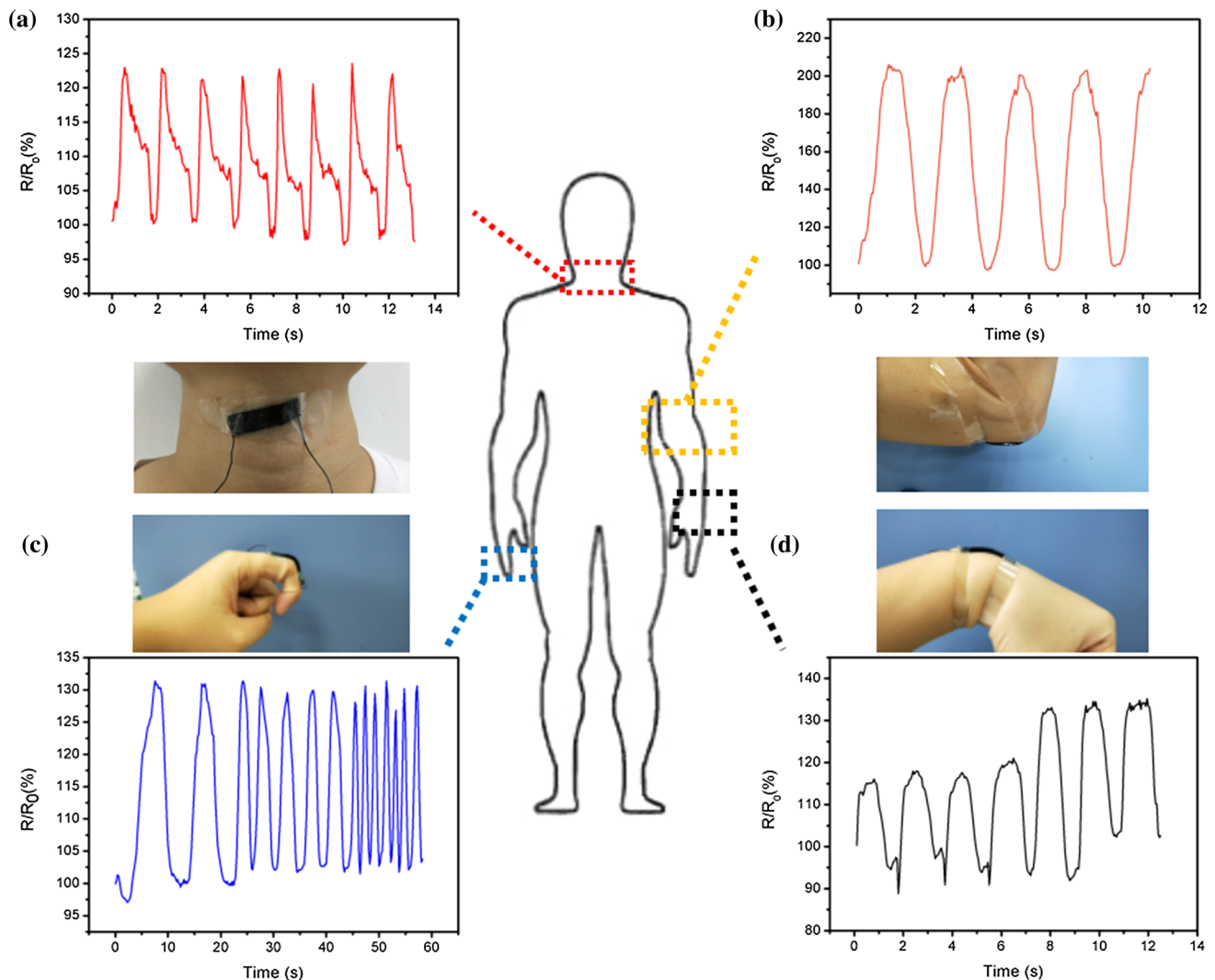


**Figure 7** a Current variations of the sensor attached to the throat induced by drinking water. Relative resistance variations of the sensor attached on the index elbow (b), the finger (c), and the opisthenar (d) induced by bending.

pathways in the stretched state may also contribute to increase in the response (Fig. 8e). The stretchable HCT hydrogel-based light-sensitive sensor is advantageous over conventional rigid light-sensitive sensor that has fixed device structures and unchangeable sensitivity. The remarkable stretchability, high sensitivity and self-healing ability make the HCT hydrogels a promising light-sensitive material.

### Self-healing and rebuilding ability

To prove that the HCT hydrogels have excellent self-healing properties, the HCT hydrogel is connected with an analyzer and a LED bulb in the circuit (Fig. 9a). First, the LED bulb is lighted by a 2v power in the circuit. After cutting the HCT hydrogel by a

blade, the LED bulb go out in the open circuit (Fig. 9b). As shown in Fig. 9c, when the two parts are connected, the LED bulb lights up again after self-healing via the reformed dynamic cross-linking between the two parts contact interfaces. To further investigate the self-healing property of HCT hydrogels and the recovery of their conductivity, HCT hydrogel was connected with the real-time resistance measurement system. Figure 9d shows the time evolution of real-time resistance variation in HCT hydrogel during typical electrical self-healing process. After the healable HCT hydrogel is cut off, the resistance changes from a steady state to infinity. When the two sections of the hydrogel are put together, the resistance drops rapidly and quickly restores to its original level. Due to the advantages of high

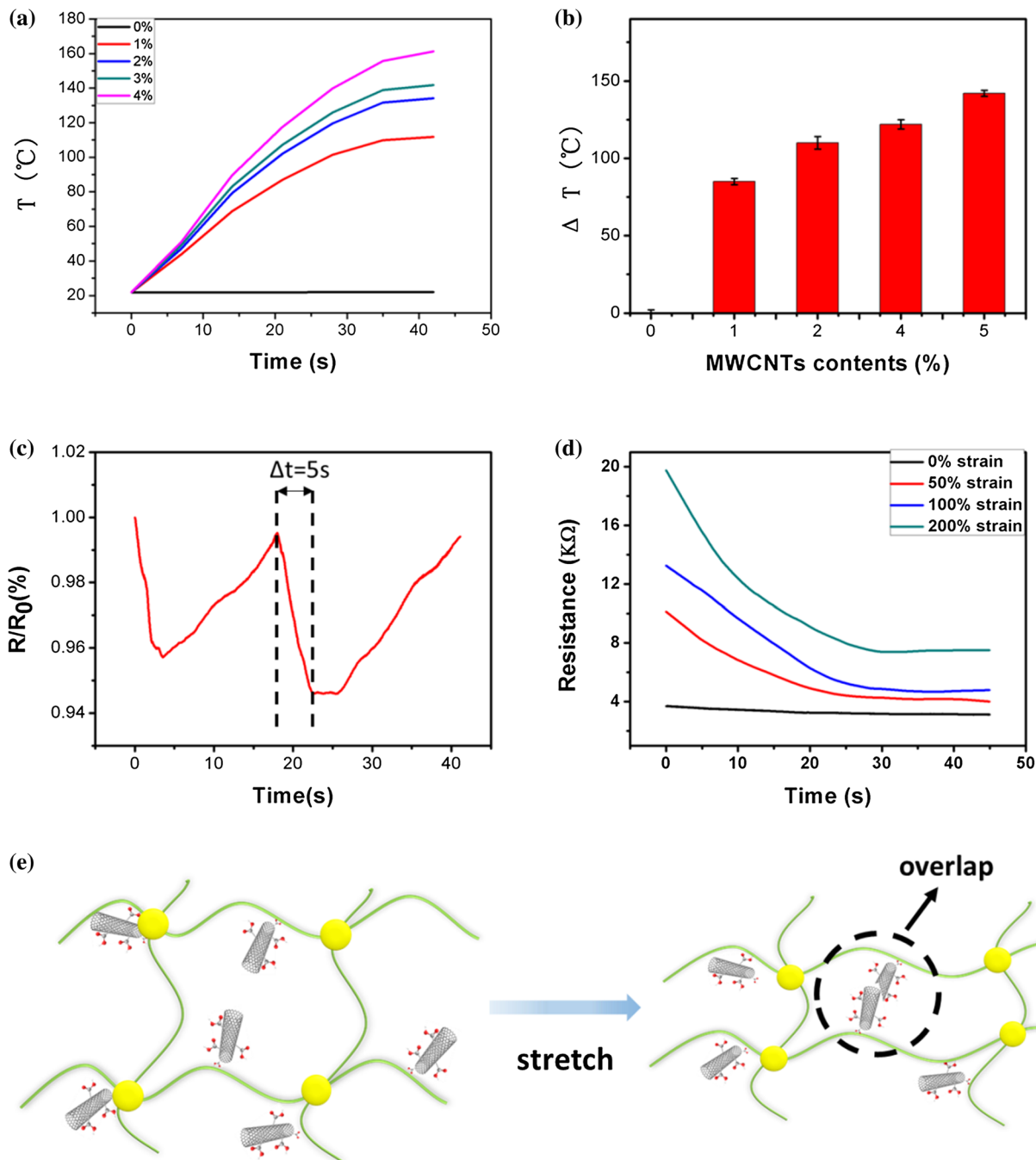


**Figure 8** **a** The temperature variations of HCT hydrogels with different MWCNTs contents under near-infrared laser irradiation; **b** the temperature changes of HCT hydrogel with different MWCNTs contents; **c** the relative resistance variations of HCT

hydrogel under near-infrared laser irradiation and the response time ( $\Delta t$ ); **d** the resistance variations of HCT hydrogel at different strain deformation under near-infrared laser irradiation; **e** microstructure model of HCT hydrogel before and after strain.

self-healing efficiency and rapid self-healing ability, HCT hydrogel can be used to construct self-healing electronic devices, bioelectronic sensors and electronic skin.

As shown in the Fig. 9e, HCT hydrogel is cut into small particles which average diameter is 1 mm, then put the particles in the designed rubber mould and place them under normal temperature for 1 d. After removing the hydrogel from the mould, a complete

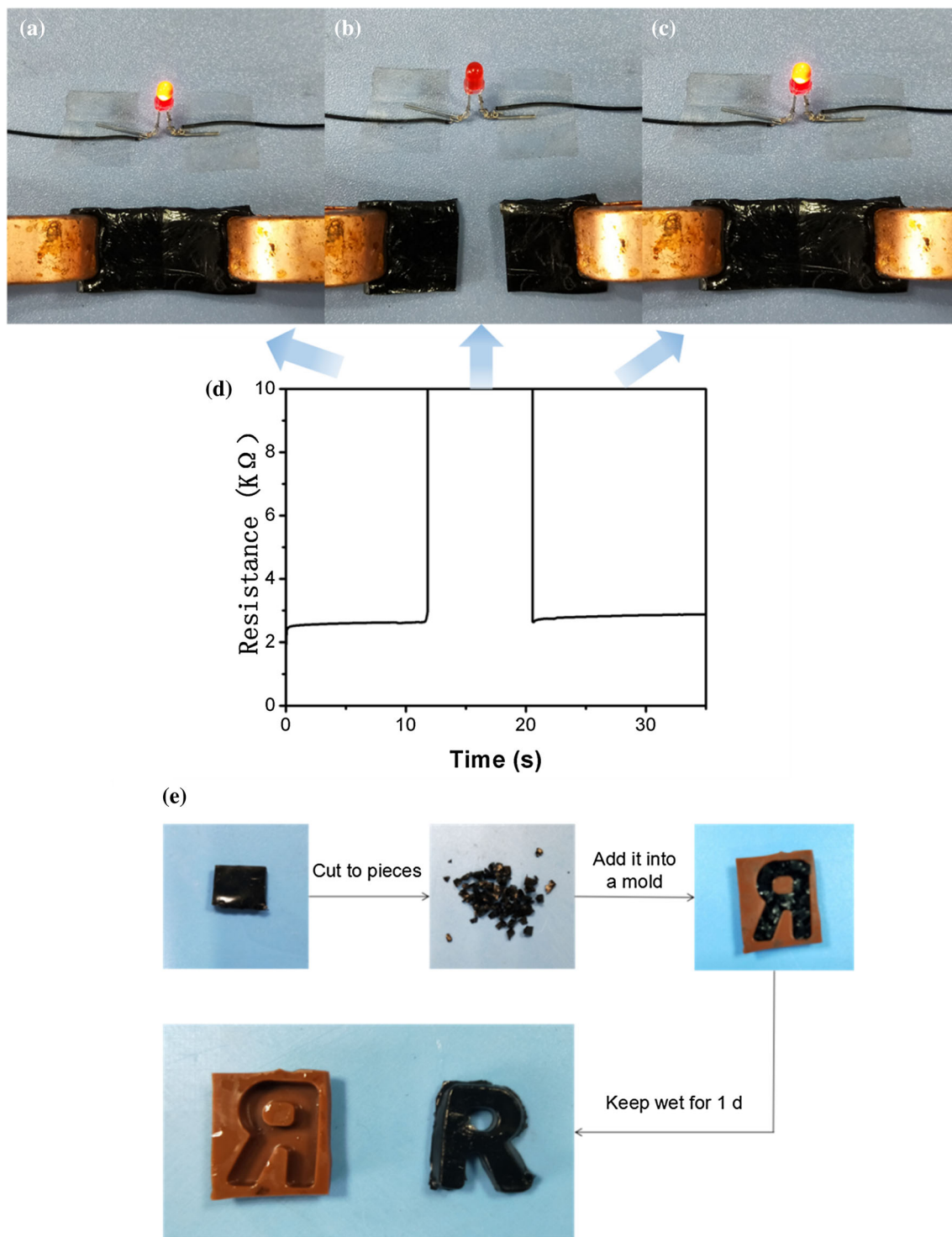


**Figure 9** The changes for LED light in the circuit before cutting (a), before self-healing (b) and after self-healing (c); **d** the variations for the sensing performance of the HCT hydrogel before and after self-healing; **e** reshape process of HCT hydrogel.

hydrogel without any crack was obtained, because the hydrophobic-associated hydrogels have robust dynamic physical cross-linking and hydrogen bonding interaction. When the interfaces of the HCT

hydrogel adhere to each other, the hydrogen bond and dynamic physical bond will be recombined and show the excellent self-healing ability. Furthermore, we could take advantage of this excellent self-healing

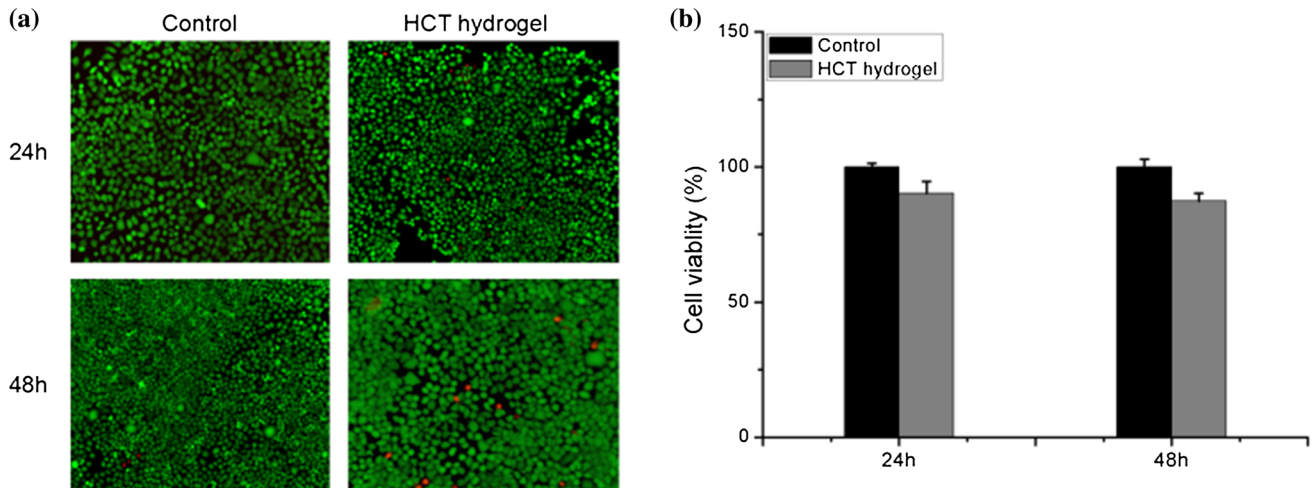


**Figure 10** **a** Fluorescent microscopy images of myocardial cells after 24 h and 48 h of incubation with regular culture medium and HCT hydrogel, scale bars: 100  $\mu\text{m}$ , **b** cell viability of myocardial

cells measured by CCK-8 assay after incubation with regular culture medium and HCT hydrogel.

ability to reshape the flexible hydrogel and get more complex 3D samples like human cartilage. It can be applied to the bionic materials which need flexible and complex hydrogel shape.

### Cytocompatibility of the hydrogel

Cardiomyocytes are chosen for cytocompatibility evaluation of HCT hydrogels by using the direct contact method, and the cell toxicity of the hydrogels was evaluated by CCK-8 assay. It is obvious that most of the cells were alive after 2 days of culture (red indicates that the cells were dead and green indicates that cells were alive), and live cells showed normal morphology. As seen in Fig. 10a, the cardiomyocytes viability was at 87.44 per cent after 48-h incubation. These results indicated no toxicity of HCT hydrogels for cardiomyocytes *in vitro*. The quantitative proliferation of myocardial cells was investigated by CCK-8 assay (Fig. 10b). This result indicated that hydrogels do not negatively affect the cell adhesion. In summary, HCT hydrogels showed good cytocompatibility *in vitro*.

### Conclusions

In this paper, we successfully prepared the multifunctional conductive HCT hydrogels through incorporating MWCNTs into the hydrophobically associated polyacrylamide (HA) hydrogel. The MWCNTs used in HCT hydrogels were modified by

modified Hummers' method. The results of FI-IR and XPS tests indicated that the oxygen-containing groups were successfully grafted on the surface of MWCNTs. The flexible HCT hydrogels have a porous structure and can bear large deformation. The conductive HCT<sub>5</sub> hydrogel displayed a high conductivity of  $0.5 \text{ S m}^{-1}$ . Then, a super-sensitive strain sensor designed using HCT<sub>5</sub> hydrogel showed high sensitivity whose GF was 5.6. Also, a simple and wearable device was constructed to detect the movements of human's large and tiny motions. In addition, the HCT hydrogels have been proved of rapid and highly efficient self-healing capability. Furthermore, the HCT hydrogels were very sensitive to near-infrared (NIR) light and could increase the temperature from  $20^\circ$  to  $160^\circ$  in just 40 s, which can be used to construct a near-infrared photosensor. Cytotoxicity tests showed that the HCT hydrogels were not toxic to cardiomyocytes. All of these results indicated that these conductive and multifunctional hydrogels exhibited great potential for application in intelligent sensors, wearable electronic devices and photosensor.

### Acknowledgements

This work was supported by National Natural Science Foundation of China (Grant Nos 51773124, 51403132), Sichuan Science and Technology Program China (Grant Nos 2016GZ0300, 2018GZ0322), Innovation Team Program of Science and Technology

Department of Sichuan Province (Grant No 2014TD0002), Cooperation strategic Projects of Luzhou governments and Sichuan University (Grant No 2015CDLZ-G13) and the Fundamental Research Funds for the Central Universities (Grant No 2012017yjsy184).

## Compliance with ethical standards

**Conflicts of interest** There are no conflicts of interest to declare.

**Electronic supplementary material:** The online version of this article (<https://doi.org/10.1007/s10853-019-03438-3>) contains supplementary material, which is available to authorized users.

## References

- [1] Hammock ML, Chortos A, Tee BC, Tok JB, Bao Z (2013) 25<sup>th</sup> anniversary article: the evolution of electronic skin (e-skin): a brief history, design considerations, and recent progress. *Adv Mater* 25(42):5997–6038
- [2] Lu B, Ying C, Ou D, Hang C, Diao L, Wei Z, Zheng J, Ma W, Sun L, Xue F (2015) Ultra-flexible piezoelectric devices integrated with heart to harvest the biomechanical energy. *Sci Rep* 5:16065
- [3] Cui W, Ji J, Cai FY, Li H, Rong R (2015) Robust, anti-fatigue, and self-healing graphene oxide/hydrophobic association composite hydrogels and their use as recyclable adsorbents for dye wastewater treatment. *J Mater Chem A* 3(33):17445–17458
- [4] Yang CH, Chen B, Lu JJ, Yang JH, Zhou J, Chen YM, Suo Z (2015) Ionic cable. *Extreme Mech Lett* 2015(3):59–65
- [5] Georgakilas V, Perman JA, Tucek J, Zboril R (2015) Broad family of carbon nanoallotropes: classification, chemistry, and applications of fullerenes, carbon dots, nanotubes, graphene, nanodiamonds, and combined superstructures. *Chem Rev* 115(11):4744–4822
- [6] Vaisman L, Wagner HD, Marom G (2006) The role of surfactants in dispersion of carbon nanotubes. *Adv Colloid Interface Sci* 128(128–130):37–46
- [7] Kim JY (2009) Carbon nanotube-reinforced thermotropic liquid crystal polymer nanocomposites. *Materials* 2(4):1955–1974
- [8] Miao J, Zhang F, Lin Y, Wang W, Gao M, Li L, Zhang J, Zhan X (2016) Highly sensitive organic photodetectors with tunable spectral response under bi-directional bias. *Adv Opt Mater* 4(11):1711–1717
- [9] Kielar M, Dhez O, Pecastaings G, Curutchet A, Hirsch L (2016) Long-term stable organic photodetectors with ultra low dark currents for high detectivity applications. *Sci Rep* 6:39201
- [10] Qi J, Qiao W, Wang ZY (2016) Advances in organic near-infrared materials and emerging applications. *Chem Rec* 16(3):1531–1548
- [11] Rogalski A (2002) Infrared detectors: an overview. *Infrared Phys Technol* 43(3):187–210
- [12] Jain PK, Huang X, Elsayed IH, Elsayed MA (2010) Noble metals on the nanoscale: optical and photothermal properties and some applications in imaging, sensing, biology, and medicine. *ChemInform* 40(14):1578–1586
- [13] Yi X, Wang F, Qin W, Yang X, Yuan J (2014) Near-infrared fluorescent probes in cancer imaging and therapy: an emerging field. *Int J Nanomed* 1:1347–1365
- [14] Guo B, Glavas L, Albertsson AC (2013) Biodegradable and electrically conducting polymers for biomedical applications. *Prog Polym Sci* 38(9):1263–1286
- [15] Wang Z, Zhou H, Chen W, Li Q, Yan B, Jin X, Ma A, Liu H, Zhao W (2018) Dually synergetic network hydrogels with integrated mechanical stretchability, thermal responsiveness and electrical conductivity for strain sensors and temperature alertors. *ACS Appl Mater Interface* 10(16):14045–14054
- [16] Zhao X, Li P, Guo B, Ma PX (2015) Antibacterial and conductive injectable hydrogels based on quaternized chitosan-graft-polyaniline/oxidized dextran for tissue engineering. *Acta Biomater* 26:236–248
- [17] Wang L, Wu Y, Guo B, Ma PX (2015) Nanofiber yarn/hydrogel core-shell scaffolds mimicking native skeletal muscle tissue for guiding 3D myoblast alignment, elongation, and differentiation. *ACS Nano* 9(9):9167
- [18] Wu Y, Wang L, Guo B, Ma PX (2017) Interwoven aligned conductive nanofiber yarn/hydrogel composite scaffolds for engineered 3D cardiac anisotropy. *ACS Nano* 2017:5646–5659
- [19] Ghavaminejad A, Hashmi S, Stadler FJ (2016) Effect of H<sub>2</sub>O and reduced graphene oxide on the structure and rheology of self-healing, stimuli responsive catecholic gels. *Rheol Acta* 55(2):1–14
- [20] Zhao X, Wu H, Guo B, Dong R, Qiu Y, Ma PX (2017) Antibacterial anti-oxidant electroactive injectable hydrogel as self-healing wound dressing with hemostasis and adhesiveness for cutaneous wound healing. *Biomaterials* 122:34–47
- [21] Gong X, Tong M, Xia Y, Cai W, Ji SM, Cao Y, Yu G, Shieh CL, Nilsson B, Heeger AJ (2009) High-detectivity polymer photodetectors with spectral response from 300 nm to 1450 nm. *Science* 325(5948):1665–1667

- [22] Xia S, Song S, Gao G (2018) Robust and flexible strain sensors based on dual physically cross-linked double network hydrogels for monitoring human-motion. *Chem Eng J* 354:817–824
- [23] Wang Z, Zhou H, Lai J (2018) Extremely stretchable and electrically conductive hydrogels with dually synergistic networks for wearable strain sensors. *J Mater Chem C* 6(34):9200–9207
- [24] Lai J, Zhou H, Wang M, Chen Y, Jin Z, Li S, Yang J, Jin X, Liu H, Zhao W (2018) Recyclable, stretchable and conductive double network hydrogels towards flexible strain sensors. *J Mater Chem C* 6(48):13316–13324
- [25] Liu YJ, Cao WT, Ma MG (2017) Ultrasensitive wearable soft strain sensors of conductive, self-healing, and elastic hydrogels with synergistic “soft and hard” hybrid networks. *ACS Appl Mater Interfaces* 9(30):25559–25570
- [26] Liu S, Li L (2017) Ultrastretchable and self-healing double-network hydrogel for 3D printing and strain sensor. *ACS Appl Mater Interfaces* 9(31):26429–26437
- [27] Mredha MTI, Guo YZ, Nonoyama T, Nakajima T, Kurokawa T, Gong JP (2018) A facile method to fabricate anisotropic hydrogels with perfectly aligned hierarchical fibrous structures. *Adv Mater* 30(9):1704937
- [28] Yan C, Wang J, Lee PS (2015) Stretchable graphene thermistor with tunable thermal index. *ACS Nano* 9(2):2130

**Publisher's Note** Springer Nature remains neutral with regard to jurisdictional claims in published maps and institutional affiliations.